

# **Correction of river bathymetry parameters using the stage–discharge rating curve**

**Xudong Zhou<sup>1</sup>, Menaka Revel<sup>1</sup>, Prakat Modi<sup>2</sup>, Takuto Shiozawa<sup>1</sup>, Dai Yamazaki<sup>1</sup>**

<sup>1</sup> Global Hydrological Prediction Center, Institute of Industrial Science, The University of Tokyo, Tokyo, Japan

<sup>2</sup> Department of Civil Engineering, Graduate School of Engineering, The University of Tokyo, Tokyo, Japan

Corresponding author: Xudong Zhou (x.zhou@rainbow.iis.u-tokyo.ac.jp)

## **Key Points**

- Empirical river bathymetry approximation equations introduce bias into local water surface elevation simulations.
- Water surface elevation bias (difference between the rating curves for simulations and observations) reflects only river bathymetry bias.
- River bathymetry corrections based on the rating curve are robust, regardless of runoff uncertainties and discharge errors.

## **Abstract**

River bathymetry is an important parameter for hydrodynamic modeling; however, it is associated with large bias because direct large-scale measurements are impractical. Recent studies adjusted river bathymetry data based on assessment of the difference between modeled and observed water surface elevation (WSE); however, model uncertainties in river discharge can lead to unintended errors in correcting river bathymetry. In this study, we propose a simple but robust correction method using the WSE bias, based on stage–discharge rating curves rather than time series data. The rating curve represents the characteristics of the river section, and is not sensitive to the instantaneous simulated discharge errors. Our results showed that the “corrected river bathymetry” converged among discharge experiments driven by noise-corrupted or multi-model runoff forcing. Evaluation with the corrected river bathymetry against virtual truth demonstrated that the new method reduced 0.85-1.12 m of the absolute bias than result from the conventional method. The deviation in the results is only 20-30% of that by the conventional method. Given the difficulty of

eliminating discharge errors and bias in runoff, a method for correcting river bathymetry that is free from discharge and runoff errors is important for improving hydrodynamic modeling.

### **Plain Language Summary**

Errors in modeled river discharge and river bathymetry affect the accuracy of water surface elevation (WSE) simulations. Comparison of simulated and observed WSEs can help quantify such errors. However, conventional methods for assessing bias in WSE time series data cannot discriminate the error sources. In this study, we propose a simple method for evaluating WSE bias based on stage–discharge rating curves. The rating-curve based WSE bias is insensitive to runoff and discharge, and can be applied to correct river bathymetry. Our results showed that river bathymetry corrections were similar regardless of the amount of runoff error, i.e., the corrections were independent of river discharge modeling errors. Accurately modeling discharge is challenging due to climate forcing, model complexity, inhomogeneity of model parameters, and the difficulty of representing human interventions. Therefore, a robust method for correcting river bathymetry in hydrodynamic models, which is independent of river discharge bias, is required.

**Key words:** Bias correction, rating curve, river bathymetry, water surface elevation

## 1 Introduction

Water surface elevation (WSE) is used for the evaluation of river flow regimes, flood risk, and riparian ecosystems, and is also applied in biodiversity studies (Sauer et al., 2021). Although space observation satellites (e.g., ENVISAT, JASON, ICESat, and SARAL) have significantly improved WSE data coverage and accessibility (Musa et al., 2015), obtaining spatially and temporally continuous WSE data at large scales is feasible only through hydrodynamic modeling. In hydrodynamic modeling, river bathymetry is a key factor for accurate simulation (Brêda et al., 2019; Yoon et al., 2012), especially for WSE. Therefore, achieving higher-accuracy river bathymetry is the goal of this study.

Direct measurement of underwater topography is impractical at large scales (Schaperow et al., 2019; Yoon et al., 2012; Zhang et al., 2011). The latest global river models, such as CaMa-Flood (Yamazaki et al., 2011) and LISFLOOD-FP (Neal et al., 2012), approximate river bathymetry based on a power-law relationship with climatological discharge. Power law-based bathymetry can capture large-scale patterns of river discharge and inundation (Di Baldassarre et al., 2009; Hirabayashi et al., 2013; Zhou, Prigent, et al., 2021), but some local calibration is required, including comparison with cross-section data and assessment of uncertainty in bathymetry parameters (Yamazaki et al., 2012).

The correction of bathymetry parameters in large-scale hydrodynamic models is a widely studied problem in hydrology. Bathymetry is typically corrected based on riverbed elevation bias (Revel et al., 2020); this process relies on observed WSEs (synthetic values or *in situ* and satellite-based observations) and high-quality model simulations of water depth. However, in many studies, simulated river discharge contained errors (Moramarco et al., 2019; Oubanas et al., 2018), resulting in errors in subsequent water depth simulations and river bathymetry correction. Brêda et al. (2019) and Jiang et al. (2019) calibrated discharge simulation models before applying them to bathymetry correction. Oubanas et al. (2018), Pujol et al. (2020) and Yoon et al. (2012) used data assimilation to simultaneously correct various biases, even in complex models with high computation costs. However, although simulated river discharge bias has been decreased through these methods, this bias (and associated uncertainties) cannot be eliminated. The robustness of bathymetry correction therefore remains in question. Thus, a robust bathymetry correction method that is not affected by errors in river discharge is needed.

The stage–discharge rating curve represents the relationship between water stage and river

discharge at a specific river cross-section (Di Baldassarre & Montanari, 2009; King et al., 2018); it is primarily determined by river characteristics including bathymetry, rather than the instantaneous river discharge (WMO, 1994). Comparison of the rating curves of model simulations and observations can be applied to avoid instantaneous discharge error and extract important information for correcting river bathymetry.

Therefore, in this study, we developed a method that utilizes the rating curve to correct river bathymetry for a global hydrodynamic model. Compared to conventional correction approaches, this method is independent of river discharge errors. The methods and data, including the descriptions of the new method, the experimental design and the study area, will be presented in the second section. Results are presented in the third section, and three subsections correspond to three different experiments. The discussions and conclusions are followed as the last two sections.

## 2 Methods and data

### 2.1 Hydrodynamic models

In this study, we used the Catchment-based Macro-scale Floodplain (CaMa-Flood) model for hydrodynamics simulations (i.e., river discharge and WSE), and for river bathymetry correction. CaMa-Flood obtains information on river hydrodynamics via shallow water equations and sub-grid topography parameterization. Its accuracy is highly dependent on the quality of the topography parameters, such as floodplain elevation, river channel depth, and river channel width. Floodplain elevation and channel width are measured by satellites (refer to MERIT DEM, GWD-LR, and MERIT Hydro, Yamazaki et al., 2017, 2015, 2019), whereas channel depth (a default model setting) is approximated by an empirical power-law function of river discharge:

$$B = \max (B_{min}, c_B * Q_{ave}^{p_B}) , \quad (1)$$

where  $B$  is the channel depth (m), and  $Q_{ave}$  is the annual average discharge ( $\text{m}^3 \text{s}^{-1}$ ). The other constants in Eq. (1) are based on “best practices”:  $B_{min} = 1.0$ ,  $c_B = 0.1$ , and  $p_B = 0.5$ . CaMa-Flood and its parameter settings have been described in detail elsewhere (Yamazaki et al., 2011).

### 2.2 Bias calculation

#### 2.3.1 Time Series Method (TS-Method) and Time Series Bias (TSB)

Power law approximations of channel depth contain local errors for certain river reaches. Therefore, river bathymetry correction based on estimated WSE bias should be applied, under the assumption that bathymetry and WSE bias are equal (i.e., changes in WSE follow those in riverbed elevation). The conventional method estimates WSE bias directly by averaging the differences between WSE simulations and observations in the time series: we term this bias TSB (Fig. 1a, 1b).

$$TSB = \frac{1}{T} \sum_{t \in T} TSB_t = \frac{1}{T} \sum_{t \in T} (WSE_{sim,t} - WSE_{obs,t}), \quad (2)$$

where  $WSE_{sim,t}$  is the WSE simulated by the model at time  $t$  and  $WSE_{obs,t}$  is the WSE observed at time  $t$ . Only time steps with available observations ( $t \in T$ ) are counted.  $T$  is the total number of samples, and TSB is the mean of  $TSB_t$ . The estimated TSB will be used to correct the river bathymetry, and the bias correction using TSB is named TS-Method.

### 2.3.2 Rating Curve Method (RC-Method) and Rating Curve Bias (RCB)

However, TSB does not have a single source of bias because WSE simulations are affected by factors including the bathymetry and simulated river discharge. To overcome this limitation, we propose the new metric RCB, which is calculated using rating curves that describe the relationship between WSE and the discharge time series (Fig. 1c). We assumed WSE can be approximated by a power-law function of river discharge (Eq. 3 and 4). A pair of functions are prepared for observations and simulations, by calibrating parameters ( $b$  and  $h$ ).

$$f_{obs} = Q_{obs}^{b_0} + h_0, \quad (3)$$

$$f_{sim} = Q_{sim}^{b_1} + h_1, \quad (4)$$

where  $f$  is the water surface elevation that corresponds to  $Q$ .  $f$  can be  $f_{obs}$  for observations (Eq. 3) or  $f_{sim}$  for simulations (Eq. 4).  $Q$  can be river discharge for observations ( $Q_{obs}$ ) or simulations ( $Q_{sim}$ ). The parameters  $b_0$ ,  $b_1$ ,  $h_0$  and  $h_1$  are constants and calculated using the least-squares method. Thus, RCB is the difference between two fitted rating curves for simulations and observations (Fig. 1c).

$$RCB = \frac{1}{T} \sum_{t \in T} RCB_t = \frac{1}{T} \sum_{t \in T} (f_{sim}(Q_{obs,t}) - f_{obs}(Q_{obs,t})). \quad (5)$$

RCB reflects the WSE bias only when the discharge is identical in both curves; therefore, RCB is independent of river discharge errors, including biases and uncertainties. Due to errors in the simulated discharge, the estimated RCB is expected to differ from TSB; their difference is attributed to discharge errors. The bias correction based on the RCB is named RC-Method.

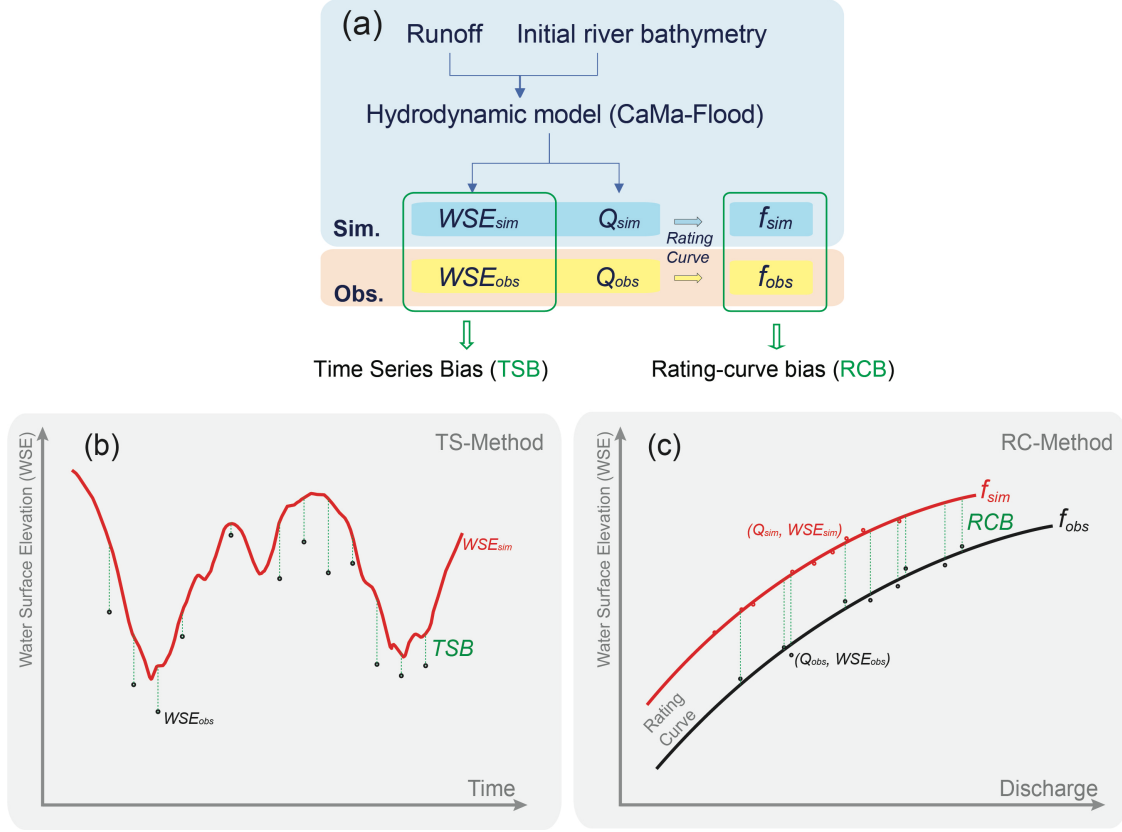


**Figure 1 Schematic diagrams of the two bias correction methods. (a)** Flow chart of estimating TSB and RCB. **(b)** Diagrams of the TS-Method with a sample time series of WSE observed (black dots) and model-simulated (red line) WSE. TSB is calculated between  $WSE_{sim}$  and  $WSE_{obs}$  when observations are available. **(c)** Diagrams of the RC-Method. Black and red fitting curves are rating curves for simulations ( $f_{sim}$ ) and observations ( $f_{obs}$ ), respectively. RCB is calculated as the difference between  $f_{sim}$  and  $f_{obs}$  when observations are available.

### 2.3 River bathymetry correction

Next, WSE data estimated using the TS-Method or RC-Method are applied to correct river bathymetry parameters. The WSE bias will be attributed to the river bathymetry bias. Thus, the estimated bias at a station (i.e., where both water altimetry and river discharge are measured) was used directly to correct river bathymetry at that point (e.g.,  $\Delta Y_{N1}$  and  $\Delta Y_{N2}$  in Fig. 2a). Corrections in river segments between the stations were done by linear interpolation according to the segment length (e.g.,  $\Delta Z_i$  and  $\Delta Z_{i-1}$ ; Fig. 2b). These corrections were applied by modifying the initial river bathymetry (red line in Fig. 2c) to the corrected river bathymetry (dark blue line in Fig. 2c). We assumed a bias correction of zero at the river mouth as no downstream data were available and

interpolation started at higher-order rivers (lower mainstream), followed by tributaries. Extrapolation was not applied to upstream regions without stations.

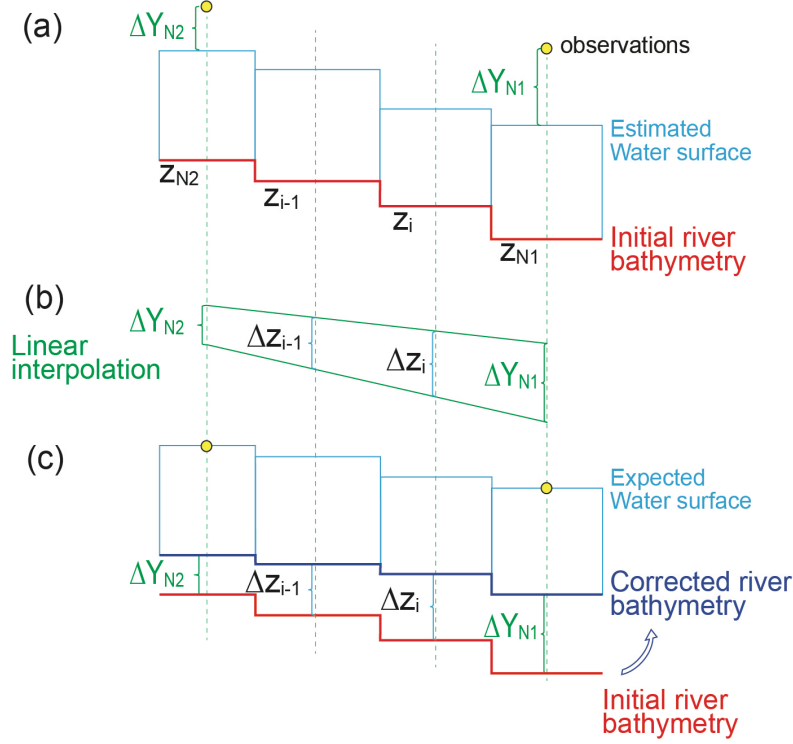


**Figure 2 Schematic diagrams of the river bathymetry correction with linear interpolation.**

**(a)** The initial status and comparison with observations. **(b)** Calculation of bias in river segments between gauges with linear interpolation. **(c)** Correction of the river bathymetry with calculated biases.

## 2.4 Experimental design

River discharge errors are the result of many factors including climate forcing, rainfall runoff generation, and river routing. Assessment of error sources was beyond the scope of the present study, which aimed to confirm the applicability and robustness of the proposed method. Accordingly, we prepared a few sets of river discharge data showing spatial and temporal variation to represent certain types of river discharge error. Thus, CaMa-Flood was driven by various runoff inputs, leading to variation in river discharge. Specifically, we designed the following three experiments:

- (1) Experiment with noise-corrupted runoff inputs. We used runoff data from the E2O

WRR2 project, which were simulated using the ECMWF HTESSEL land surface model (Balsamo et al., 2009) as the baseline runoff data for this study. Then, we prepared four perturbed runoff inputs ( $-50\%$ ,  $-25\%$ ,  $+25\%$ , or  $+50\%$  compared to baseline runoff). The initial river bathymetry was calculated using an empirical equation (Eq. 1), as the default setting of the CaMa-Flood model. CaMa-Flood was then driven by the five runoff inputs using the same initial river bathymetry. TSB and RCB were calculated against observations and compared among the five parallel runs. River bathymetry was corrected using the TS-Method and RC-Method. The model simulations and estimated bias were updated based on the corrected river bathymetry to evaluate the correction efficiency.

(2) Experiment with multiple model-based runoff inputs. More than using noise-corrupted runoff, we applied more reasonable runoff error ranges in multiple models used to simulate earth2Observe project data (Schellekens et al., 2017). These runoff are driven by same forcing inputs (WATCH Forcing Data methodology applied to ERA- Interim data, WFDEI; Weedon et al., 2014) while using different hydrological/land surface models. In short, they are named as anu, cnrs, jrc, ecmwf, nerc, univk and univu, identified by the host institution of each product. The other processes remain the same as the previous experiment. The model-based runoff inputs are with smaller differences, albeit with more complex spatiotemporal patterns than the noise-corrupted runoff inputs.

(3) Observing system simulation experiments (OSSEs). In the above experiments, we were unable to evaluate the accuracy of the corrected river bathymetry due to a lack of actual river bathymetry data. Therefore, we use OSSEs (Andreadis et al., 2007) to test if the correction of river bathymetry is accurate compared to a virtual river bathymetry. Specifically, we firstly ran CaMa-Flood using the baseline runoff (i.e., ECMWF) and the virtual true river bathymetry (i.e., corrected river bathymetry in the first experiment with ECMWF input and RC-Method). The outputs of the river discharge and water surface elevation from CaMa-Flood are treated as the virtual observations. Afterwards, we re-conducted the second experiment, as that seven model simulated runoffs from the earth2observe project are used as runoffs with unknown biases and uncertainties. Then CaMa-Flood was run with the initial river bathymetry (default with empirical equation) and various runoff inputs for simulations of discharge and water surface elevation. While, the simulations were evaluated with the virtual observations, rather than the real-world observations (GRDC and HydroWeb), to obtain the two biases (i.e., TSB and RCB). The initial river bathymetry



was then corrected with the TSB and RCB. The correction performance was evaluated against the virtual true river bathymetry prepared in the previous step. Ideally, the corrected river bathymetry should overlap the virtual true bathymetry.

## 2.5 Study area and other settings

River discharge data were obtained from the Global Runoff Data Centre (GRDC; <https://portal.grdc.bafg.de>) and WSE data were extracted from HydroWeb (<http://hydroweb.theia-land.fr>). We limited the study area to the Amazon region, for which large amounts of GRDC and HydroWeb satellite altimetry data are available. A virtual station is defined as the intersection between a satellite theoretical track and a river centerline. We only considered unit catchments (the basic unit of CaMa-Flood) containing both virtual station (altimetry measurements) and GRDC station (discharge observations). Although the two stations are not necessarily overlap at the exact same location, the change in river discharge within a unit-catchment is negligible. The location is therefore location of the virtual station (Fig. 3). We wanted to test the method using large rivers, so used 20 gauges with an average discharge of  $> 5,000 \text{ m}^3 \text{ s}^{-1}$ . The study period was 2000–2010, when river discharge and HydroWeb data showed the most overlap.

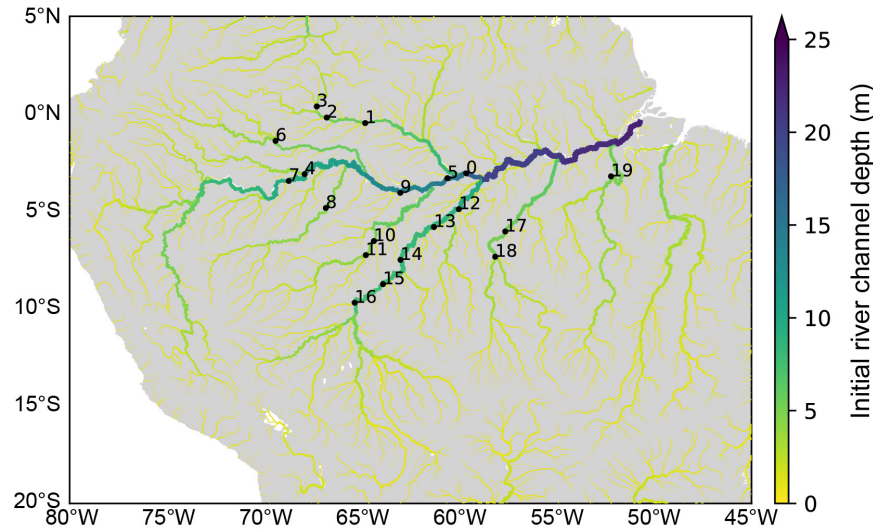


**Figure 3 The location of the selected virtual stations in the Amazon River Basin.** The Initial River channel depths was approximated using the empirical power law equation (Eq. 1). River segments with depths of  $< 2.5 \text{ m}$  were filtered out.

Besides the two TSB and RCB, we also used some other performance metrics to evaluate the simulations. These are (1) Bias in percentage, (2) Root Mean Square Error (RMSE), (3) Nash Sutcliffe Efficiency (NSE) and (4) ratio of RMSE to mean (rRMSE). The equations are given as following:

$$Bias = \frac{\sum_{t=1}^T (S_t - O_t)}{\sum_{t=1}^T (O_t)} \times 100\%, \quad (6)$$

$$RMSE = \sqrt{\frac{\sum_{t=1}^T (S_t - O_t)^2}{T}}, \quad (7)$$

$$NSE = 1 - \frac{\sum_{t=1}^T (S_t - O_t)^2}{\sum_{t=1}^T (O_t - \bar{O})^2}, \quad (8)$$

$$rRMSE = \sqrt{\frac{\sum_{t=1}^T (S_t - O_t)^2}{T}} / \bar{O}_t. \quad (9)$$

Where  $S_t$  is the simulation and  $O_t$  is the observation at timestep  $t$ . The investigated variable can be either river discharge or WSE, however, the selection of comparison pair depends on whether it is for the time series or for the rating curve.  $T$  is the total number of timesteps with both values in simulation and observation.  $\bar{O}_t$  is the mean of the observations.

### 3 Results

#### 3.1 Experiment with noise-corrupted runoff inputs

##### 3.1.1 Overview of simulations and observations

Figure 4 compares the simulations (discharge, WSE) and observations (GRDC, HydroWeb) for an example of gauge 7 (Sao Paulo De Olivenca). Only cases with three runoff inputs (baseline,  $-50\%$ , and  $+50\%$ ) are shown; the remaining two inputs were expected to fall within the range of  $-50\%$  to  $+50\%$ . Noise-corrupted runoff led to large deviations in discharge (Fig. 4a) and WSE (Fig. 4c) and the TSB of WSE varied by runoff input. WSE simulations with noise-corrupted runoff ( $-50\%$ ) had lower bias than HydroWeb (Fig. 4d), while discharge simulations driven by baseline runoff had lower bias than the GRDC data (Fig. 4b). In contrast, rating curves with different runoff inputs overlapped well (Fig. 4e). Variable runoff affected only the range of the fitting curves, indicating that they were independent of the runoff inputs. Thus, the estimated RCB did not differ by runoff input.

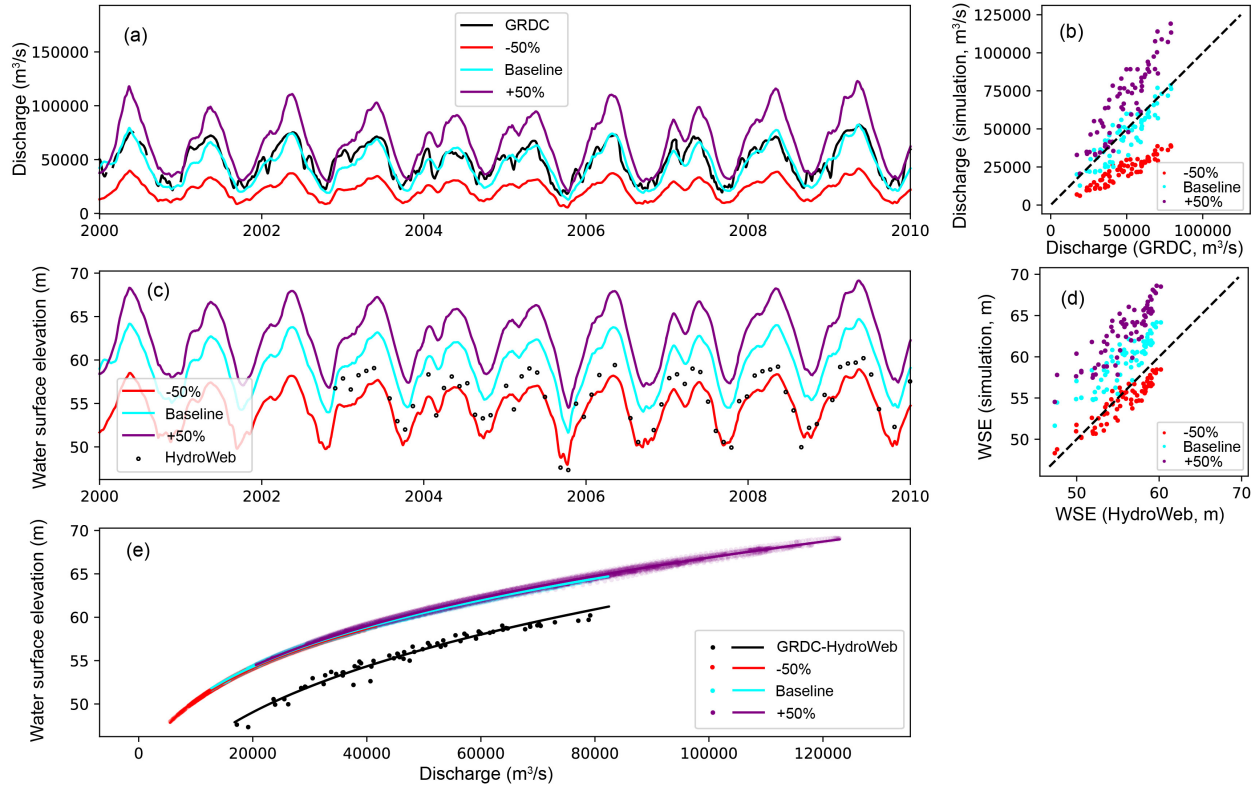


**Figure 4** Comparison of model simulations and observations for (a, b) time series river discharge data, (c, d) WSE, and (e) rating curves for gauge 7 (San Paulo De Olivenca, Amazon River). Solid lines in (e) are the rating curves fitted to observations (color) and simulations (black).

### 3.1.2 Bias calculation

The WSE biases for the 20 selected gauges were estimated using the TS-Method and RC-Method for five noise-corrupted runoff inputs (Fig. 5a). For most gauges, differences in RCB among the five runoff inputs were negligible compared to the TSB variation, indicating independence between RCB and runoff. Among all gauges, RCB showed the largest variation for gauge 12 (Fazenda Vista Alegre, Madeira River). This gauge is in a lower tributary (estimated riverbed elevation, 7.9 m; Fig. 3) where the backwater effect of the Amazon mainstem is strong. The simulations yielded a looped rating curve (Fig. S2e), such that it was not appropriate to apply a simple exponential fitting curve (Eq. 3). The riverbed is lower at gauges 0 and 5, and the hysteresis of the two gauges was likely due to the diffusive nature of the flood wave, rather than the backwater effect. River bathymetry bias estimates for specific gauges were linearly interpolated to the river segments. Figure 5b shows an example correction using baseline runoff

and the RC-Method. The corrections for all five runoff inputs are shown in Fig. S3 for both methods. Bias correction performed using the TS-Method revealed an increase in bias from lower to higher runoff levels (left column in Fig. S3). However, this was not observed when the RC-Method was applied (right column in Fig. S3).

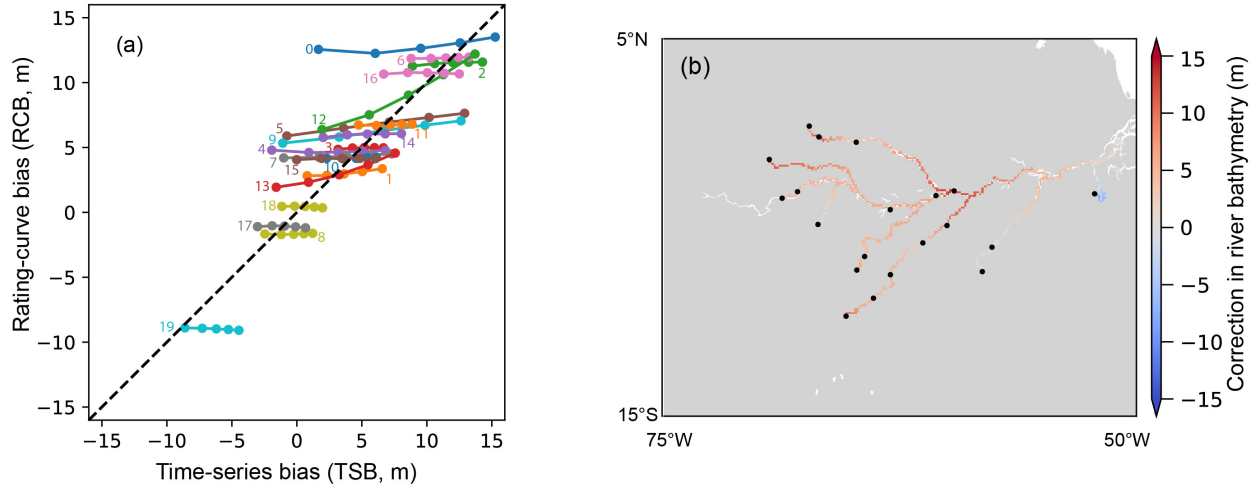


**Figure 5 (a)** Comparison of the TSB- and RCB-based river bathymetry correction methods with noise-corrupted runoff. Five dots represent results based on five runoff inputs (left to right,  $-50\%$ ,  $-25\%$ , baseline,  $+25\%$ , and  $+50\%$ ). **(b)** A sample of correction for baseline runoff using the RC-Method.

River bathymetry data for a sample tributary with five different runoff inputs corrected using the TS-Method and RC-Method are shown in Fig. 6a and 6b, respectively. For the noise-corrupted runoff, river bathymetry corrected using the TS-Method showed wide variation (blue lines, Fig. 6a), indicating high sensitivity to runoff inputs. In contrast, river bathymetry corrections using the RC-Method converged, especially for gauges 14–16 and their connecting river segments (Fig. 6b). These segments had higher riverbeds so were barely affected by backwater. A difference in river bathymetry correction was observed between gauges 12 and 13 due to the backwater effect. In conclusion, river bathymetry corrected using the RC-Method was insensitive to runoff inputs in river segments without the backwater effect, but not in those where the backwater effect was present.

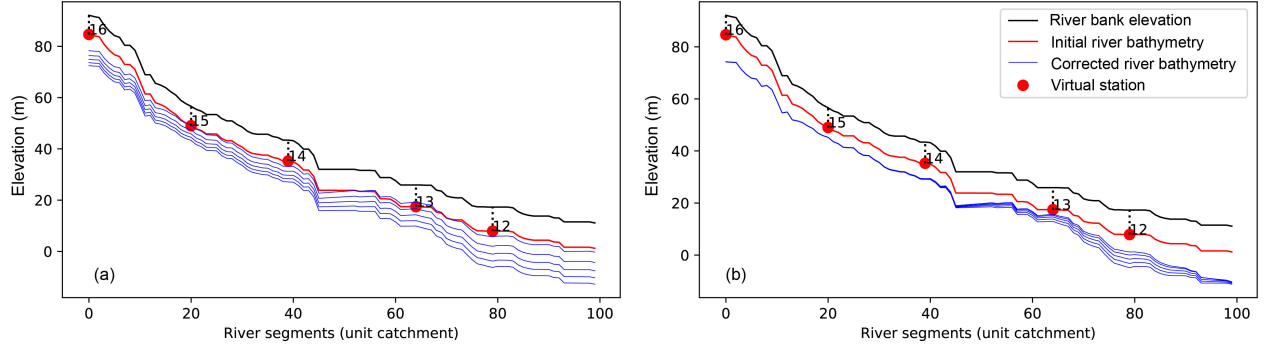


**Figure 6** River bathymetry corrections using the **(a)** TS-Method and **(b)** RC-Method for different noise-corrupted runoff inputs.

### 3.1.3 Model evaluation for corrected river bathymetry

We reran CaMa-Flood using the corrected river bathymetry and corresponding runoff. Model performance was evaluated against the observed discharge and WSE. We compared the initial experiments with those including bias corrections obtained by the TS-Method and RC-Method. The model runs are compared in bias (Fig. 7). The RMSE and Nash-Sutcliffe efficiency (NSE) results are shown in Figs. S4 and S5.

We observed large variations in river discharge depending on the runoff inputs (Fig. 7a1-7a3,  $\sim 1.8\%$ ,  $s.d.=36\%$ ). The magnitude and direction of the bias was the same between the initial runs and after bias-correction, indicating that river discharge was not significantly affected by changes in river bathymetry. Although discharge was underestimated by around 50% when using the noise-corrupted runoff input ( $-50\%$ ), the river bathymetry bias compensated for this, such that the TSB of WSE was lowest among the five runoff inputs in the initial experiments (first boxplot in Fig. 7b1). This small TSB indicated that the model was relatively unbiased, which does not accord with the underestimated river discharge. The simulations corrected via the TS-Method (Fig. 7b2) efficiently decreased the mean TSB and its deviation for all runoff inputs (1.26 m,  $s.d.=0.86$  m). However, the correction obtained using the RC-Method degraded model performance for the  $-50\%$  runoff input compared to the TS-Method (first boxplot in Fig. 7b3). This result is reasonable because the corresponding runoff input as well as the discharge were underestimated. Based on the underestimated discharge and corrected river bathymetry, the estimated WSE should be lower than the true value, showing negative TSB. The TSB for baseline runoff decreased to the lowest level among all runoff inputs following correction using the RC-Method (middle boxplot in Fig. 7b3), indicating an improvement over the TSB estimate.

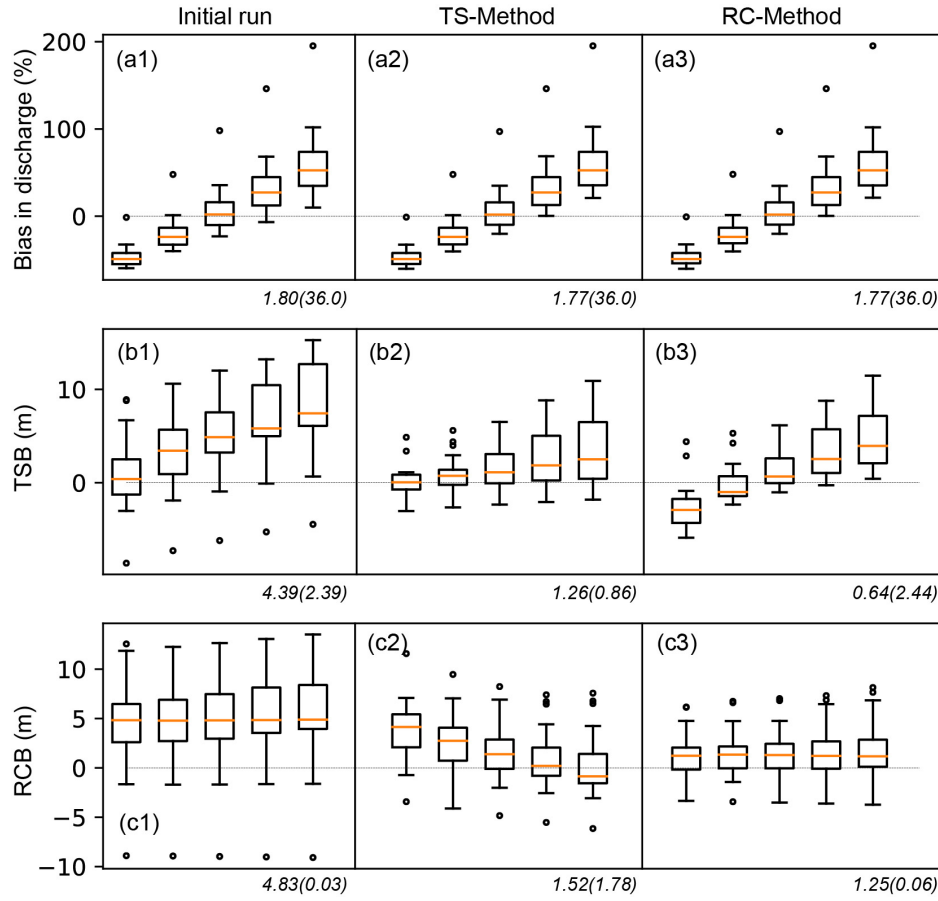


**Figure 7 Comparisons of model performance before and after applying the bias correction.**

Comparisons are conducted in terms of **(a)** discharge bias (%), **(b)** TSB, and **(c)** RCB for the initial experiments (column 1), and for simulations following river bathymetry correction using the TS-Method (column 2) and RC-Method (column 3). The five boxplots in each panel represent the five runoff inputs (left to right,  $-50\%$ ,  $-25\%$ , baseline,  $+25\%$ ,  $+50\%$ ). Boxplots were plotted based on data from 20 virtual stations. The values under each panel are the mean of the median (orange line) for different boxplots and the standard deviation in the bracket.

Unlike the initial TSB of WSE (Fig. 7b1), the RCB did not significantly differ among various runoff inputs (Fig. 7c1, 4.83 m, s.d.=0.03 m), demonstrating the independence of RCB from runoff levels. Correction using the TS-Method also reduced RCB (Fig. 7c2), although the improvements varied among runoff inputs (s.d.=1.78 m). The smallest change was observed for the lowest runoff level ( $-50\%$ ; first boxplot in Fig. 7c2) because the TSB was small due to compensation of underestimated runoff and too high river bathymetry (first boxplot in Fig. 7b1).

In contrast, overcorrection was seen for the highest runoff level (+50%; fifth boxplot in Fig. 7c2) as the positive bias became negative due to mistaken attribution of the overestimated runoff bias to river bathymetry. The updated RCB after bias-correction with RC-Method was reduced (1.25 m), and variation among runoff inputs remained low (Fig. 7c3, s.d.=0.06 m). Thus, independence of the corrected results from runoff inputs was again demonstrated, and the application of biased runoff showed similar efficiency to river bathymetry correction. Analyses based on RMSE and NSE showed the same conclusion that the performance of bias correction on the river bathymetry using RC-Method is independent from the runoff inputs (Figs. S4 and S5).

### **3.2 Experiment with multiple model-based runoff inputs**

In the first experiment, we have found that river bathymetry corrections based on RCB were not sensitive to runoff input, as shown by the convergence of corrected river bathymetry due to noise-corrupted runoff inputs. The large noise-corrupted runoff errors clearly distinguished between cases and demonstrated the independence of RCB and runoff in multiple experiments. In the second experiment, we applied more reasonable runoff from earthH2Observe project, with error ranges among multiple land-models.

The application for a sample reach is shown in Fig.8. Blue lines in Fig. 8a, representing the corrected river bathymetry by TS-Method, show a deviation driven by different runoff inputs. The variations are dominated by the runoff and show consistency from upstream to downstream. In contrast, the corrected river bathymetry converges for different runoff inputs, especially for the river segments above gauge 14 (Fig. 8b). Diverges are also seen downstream gauge 13 where backwater effects. The findings are quite similar to the experiments with the noise-corrupted runoff, although the diverges in the corrected river bathymetry are smaller with both TS-Method and RC-Method.

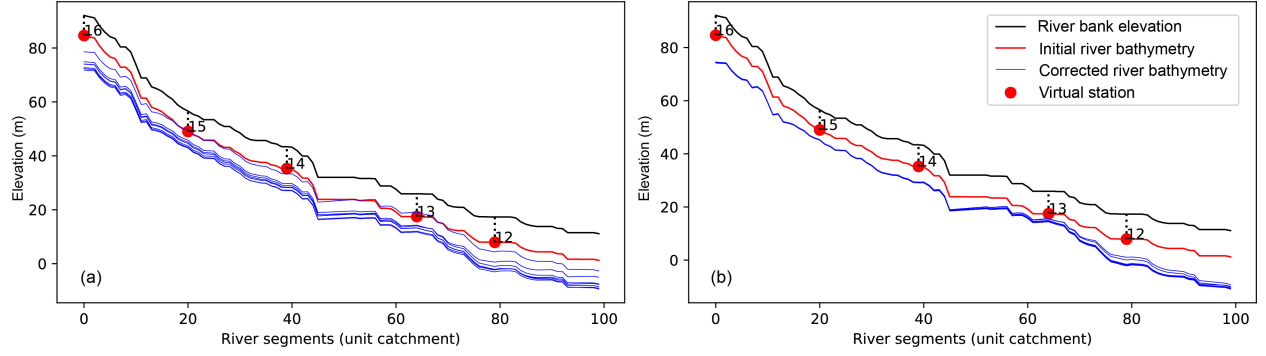


**Figure 8.** (a) and (b) illustrate the riverbank elevation, initial river bathymetry and the corrected river bathymetry with different runoff inputs using TS-Method and RC-Method, respectively. Seven different runoffs are from earth2observe project.

The biases in river discharge and WSE were also checked before and after bias correction (Fig. 9). Compared to the sequenced noise-corrupted runoff, the bias in river discharge and the TSB in WSE are smaller but less regular. The similar results for discharge bias indicate that the correction of river bathymetry still did not significantly alter river discharge (Fig. 9a1-9a3). TSB for the initial runs are varying (Fig. 9b1, 4.88 m, s.d.=1.58 m) while they are efficiently reduced after correction with TS-Method (Fig. 9b2, 2.45 m, s.d.=1.80 m). TS-Method also reduces RCB (Fig. 9c2, 3.04 m), however, the improved performance of river bathymetry is difficult to evaluate as runoff plays different roles (s.t.=1.86 m). Bias correction with RC-Method also significantly reduces the TSB (Fig. 9b3, 0.62 m), showing that the TSB is partly resulted from the bias in river bathymetry. Moreover, the magnitude of the bias can be quantified by comparing Fig. 9c1 and Fig. 9c3, showing independence between results with runoff inputs.



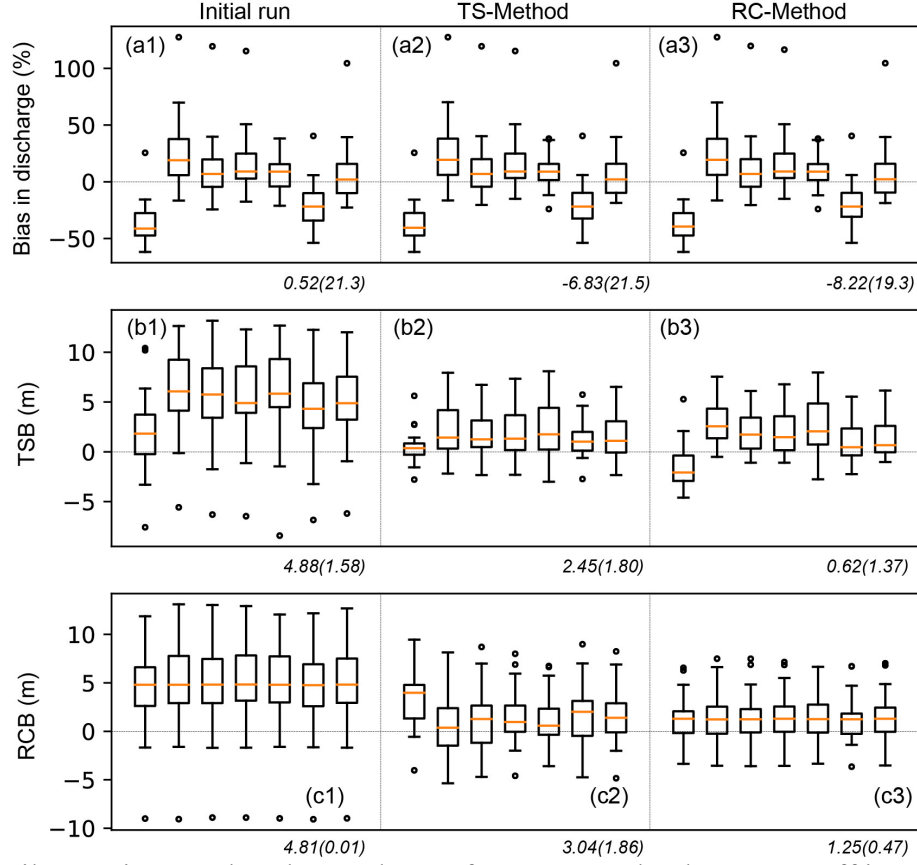


**Figure 9.** Similar to Figure 7, but the results are for seven earth2observe runoff inputs. Seven boxplots for each panel are for seven runoff inputs. Comparisons for the RMSE and NSE are similar to Figure S4 and S5, thus they are not shown. Boxplots were plotted based on data from 20 virtual stations. The values under each panel are the mean of the median (orange line) for different boxplot and the standard deviation in the bracket.

### 3.3 Observing system simulation experiments (OSSEs)

The orange dashed line in Fig. 10 represents the virtual true river bathymetry, with which we can additionally evaluate the result of bias correction. Although using the same seven runoff inputs as the second experiment, the corrected bias bathymetry are slightly different because virtual observations (i.e., simulations with virtual river bathymetry and runoff) were used instead of real observations. Nevertheless, the results with TS-Method are still diverging (Fig. 10a, mean bias 1.46 m, s.d.=2.09 m) while that with RC-Method are converging (Fig. 10b, mean bias 1.90 m, s.d.=0.36 m). Both bias correction methods are efficiently correct the river bathymetry to the target virtual true river bathymetry, while results with RC-Method show almost overlapping of the corrected and the target river bathymetry, especially above gauge 14 (mean bias 0.56 m, s.d.=0.09

m). Larger deviations are detected for lower segments with both methods, while the deviation of the bias by RC-Method (s.d.=0.56 m) is still much lower than that of the TS-Method (s.d.=2.17 m).

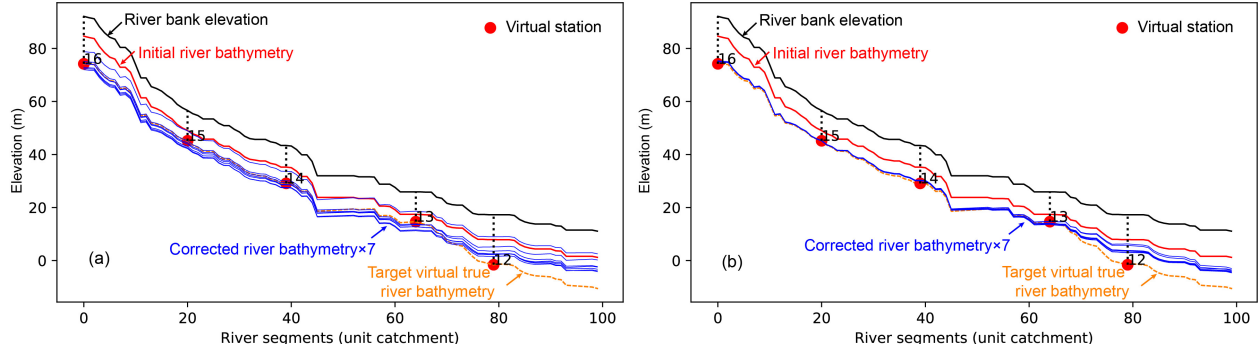


**Figure 10** Results of Observing System Simulation Experiments (OSSEs) experiment. (a) and (b) illustrate the riverbank elevation, initial river bathymetry and the corrected river bathymetry with seven different earth2observe runoff inputs using TS-Method and RC-Method, respectively. We assumed the “virtual true” target river bathymetry (orange lines). The efficiency of correction will be compared with the target river bathymetry.

The absolute bias and the RMSE are better to represent the performance as the bias contains negative value. Specifically, RC-Method provides a correction of river bathymetry in the entire river section with absolute bias 0.96 m smaller than TS-Method, and the deviation is only 22% ( $=0.31/1.43$ ) of the TS-Method. The RMSE for the entire river section is 0.72 m smaller in RC-Method, and the deviation is 31% of that with TS-Method. The apparent converging river bathymetry is seen upstream gauge 14, with smaller absolute bias (0.56 m vs. 1.68 m) and RMSE (0.63 m vs. 1.72 m), and significantly small deviations  $\sim 0.10$  m for RC-Method, but  $\sim 1.25$  m for TS-Method. Although the performance for river segments with backwater effect is worse than average, the RC-Method is providing a better bias correction than TS-Method either in the accuracy or the deviation among different runoff inputs.

**Table1** Evaluation of the corrected river bathymetry against the virtual true river bathymetry. The values represent the mean for different runoff inputs and the standard deviation in the bracket. Unit: m.

River segments	Methods	Bias	Absolute bias	RMSE
Entire river	TS-Method	1.46 (2.09)	2.93 (1.43)	3.74 (1.41)
	RC-Method	1.90 (0.36)	1.97 (0.31)	3.02 (0.44)
Upstream gauge 14	TS-Method	-0.32 (2.08)	1.68 (1.27)	1.72 (1.25)
	RC-Method	0.56 (0.09)	0.56 (0.09)	0.63 (0.08)
Downstream gauge 14	TS-Method	2.65 (2.17)	3.76 (1.60)	4.56 (1.65)
	RC-Method	2.79 (0.56)	2.91 (0.48)	3.86 (0.58)

#### 4 Discussion

In this study, we proposed a bias correction method to correct river bathymetry with the Rating Curve Bias (RCB) and compared the performance with conventional correction method by using Time Series Bias (TSB). TS-Method works well when the river discharge is well reproduced. However, precise simulation of river discharge remains challenging due to various factors such as climate forcing, complex parameterization of rainfall–runoff processes, and heterogeneity in the calculation grid. Moreover, the anthropogenic effects of water consumption and dam regulation have significantly altered natural river systems and flow regimes, increasing the complexity and difficulty of hydrological modeling (Lehner et al., 2011; Zhou, Polcher, et al., 2021). Although we reproduced river discharge errors using different runoff inputs in this study, the RC-Method has no limited applicability under the conditions described above if the main purpose of the model is to correct river bathymetry parameters. With the first step of correcting river bathymetry, more water altimetry data can be used to enhance the calibration of hydrodynamic models, especially where recent river discharge observations are not available.

The correction method proposed in this study relies on fitted rating curves. We assessed the fitting performance of CaMa-Flood simulations across the study area (Fig. 11) and observed larger rRMSE values at lower reaches and tributaries, indicating reduced accuracy; this was consistent with the differences observed in RC-Method estimates between gauges 12 and 13 (Fig. 6). The fundamental reason that simple power-law regression (Eq. 3,4) was unable to derive the looped rating curve (Fig. S2e or Fig. 11b for the gauge 12) of river reaches where the backwater effect is strong. A possible solution is to use advanced fitting curves (e.g., application of a two-

stage curve fitting method to elevations and recessions of the hydrograph and underlying curve) instead of the current fitting approach. However, we did not test advanced fitting curves in this study because, despite its limitations, the current fitting method still outperformed the TS-Method in correcting the river bathymetry in terms of the deviations (Fig. 10, s.d.=0.56 m for RC-Method and 2.17 m for TS-Method). Future studies should examine how other river channel parameters, such as the channel shape and Manning's roughness coefficient, affect the rating curve. Studies assessing errors in floodplain topography would help clarify the performance of the rating curve during high-water periods.

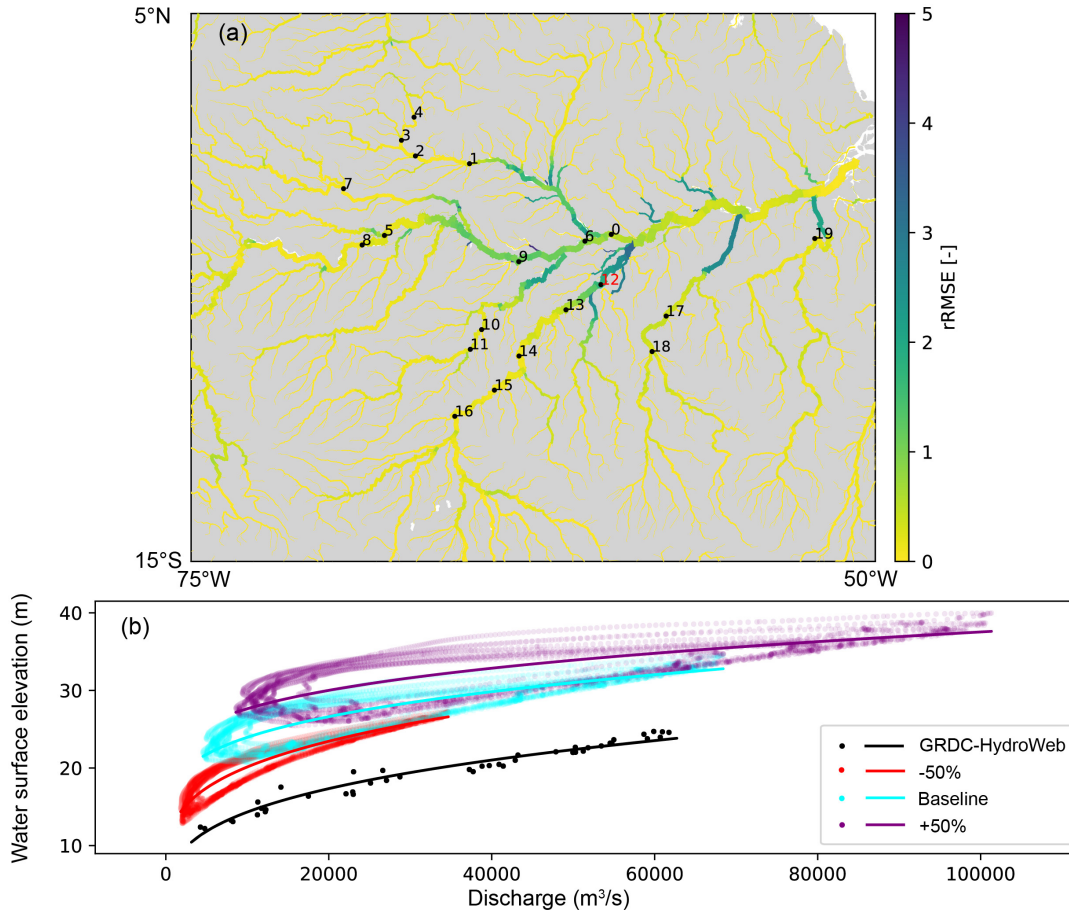


**Figure 11. (a)** The map of rRMSE (ratio of RMSE to the mean) for fitted rating curve based on CaMa-Flood simulations over the study area. It is evaluated between the simulated WSE and the WSE extracted from the rating curve. Only the unit catchments with average discharge larger than  $1000 \text{ m}^3 \text{ s}^{-1}$  are shown. The numbers represent the location of the stations to be investigated in this study. **(b)** The fitting performance of the rating curve for the noise-corrupted runoff experiments at a sample gauge 12.

We used linear interpolation for correction of river bathymetry for river segments between gauges. Although linear interpolation is less accurate than advanced approaches such as global optimal solutions or Kalman filter assimilation, Brêda et al. (2019) stated that it does not excessively degrade performance, but more efficient, and has much lower computation and time costs. The OSSEs performed in this study demonstrated good performance of the linear interpolations (Fig. 10). However, the limited availability of paired discharge–WSE observation for rivers worldwide can be a key obstacle to the application of this method. With the rapid development of multiple radar altimetry satellite missions (e.g., ENVISAT, JASON, ICESat, SARAL, and upcoming SWOT), the measurement of water altimetry has almost covered all global rivers. Accompanying with the river discharge observations from open databases (e.g., GRDC), the method can be applied to entire North America and Europe, the Amazon River basin and some specific river basins in South Africa and Australia. However, the availability of river discharge measurements has sharply decreased in the recent two decades. Therefore, a large data-sharing effort is still needed, especially of gauge discharge observations in Asian and African rivers. On the other hand, with the corrected river bathymetry, we can have a deep investigation into the optimization and regionalization of the empirical power law equation for river channel depth calculation in the hydrodynamic models. New knowledge from analysis with available data will help better implementations of the hydrodynamic models to the data-scarce regions.

## 5 Conclusion

In this study, we proposed an approach for correcting river bathymetry based on prior approximations thereof, and estimated WSE bias in hydrodynamic simulations and observations using the RCB method. The resulting river bathymetry corrections were independent of river discharge errors, as shown by the convergence of corrected river bathymetry in experiments using different runoff inputs. In comparison, the results obtained with conventional TSB-based correction of WSE estimates varied according to runoff input, and therefore were not independent of river discharge errors. Although the new method did not perform well when the backwater effect was strong, its robust independence from river discharge ensures wide applicability given that accurate river discharge modeling remains difficult due to model input biases, the complexity of model parameterization, and the increasing impact of anthropogenic effects. Thus, rating curves will become increasingly valuable as discharge and river altimetry measurements become more

widely available due to current and future satellite missions.

### **Acknowledgements:**

This study is supported by KAKENHI 20H02251 and 20K22428 by Japan Society for the Promotion of Science (JSPS), Inoue Research Award by Inoue Foundation for Science, and “LaRC-Flood project” by MS&AD Holdings.

### **Data accessibility:**

All data in this study are publicly available and were accessed at the links given above in the text (GRDC, <https://portal.grdc.bafg.de>; water altimetry data from HydroWeb (<http://hydroweb.theia-land.fr>). The global hydrodynamic model CaMa-Flood is available from Yamazaki et al. (2021). The key datasets in this study are accessible from Zhou, Revel et al. (2021).

### **Reference:**

- Andreadis, K. M., Clark, E. A., Lettenmaier, D. P., & Alsdorf, D. E. (2007). Prospects for river discharge and depth estimation through assimilation of swath-altimetry into a raster-based hydrodynamics model. *Geophysical Research Letters*, 34(10), L10403. <https://doi.org/10.1029/2007GL029721>
- Balsamo, G., Viterbo, P., Beijaars, A., van den Hurk, B., Hirschi, M., Betts, A. K., & Scipal, K. (2009). A revised hydrology for the ECMWF model: Verification from field site to terrestrial water storage and impact in the integrated forecast system. *Journal of Hydrometeorology*, 10(3), 623–643. <https://doi.org/10.1175/2008JHM1068.1>
- Brêda, J. P. L. F., Paiva, R. C. D., Bravo, J. M., Passaia, O. A., & Moreira, D. M. (2019). Assimilation of Satellite Altimetry Data for Effective River Bathymetry. *Water Resources Research*, 55(9), 7441–7463. <https://doi.org/10.1029/2018WR024010>
- Di Baldassarre, G., & Montanari, A. (2009). Uncertainty in river discharge observations: A quantitative analysis. *Hydrology and Earth System Sciences*, 13(6), 913–921. <https://doi.org/10.5194/hess-13-913-2009>
- Di Baldassarre, G., Schumann, G., & Bates, P. D. (2009). A technique for the calibration of hydraulic models using uncertain satellite observations of flood extent. *Journal of*

- Hydrology*, 367(3–4), 276–282. <https://doi.org/10.1016/j.jhydrol.2009.01.020>
- Hirabayashi, Y., Mahendran, R., Koirala, S., Konoshima, L., Yamazaki, D., Watanabe, S., Kim, H., & Kanae, S. (2013). Global flood risk under climate change. *Nature Climate Change*, 3(9), 816–821. <https://doi.org/10.1038/nclimate1911>
- Jiang, L., Madsen, H., & Bauer-Gottwein, P. (2019). Simultaneous calibration of multiple hydrodynamic model parameters using satellite altimetry observations of water surface elevation in the Songhua River. *Remote Sensing of Environment*, 225(September 2018), 229–247. <https://doi.org/10.1016/j.rse.2019.03.014>
- King, T. V., Neilson, B. T., & Rasmussen, M. T. (2018). Estimating Discharge in Low-Order Rivers With High-Resolution Aerial Imagery. *Water Resources Research*, 54(2), 863–878. <https://doi.org/10.1002/2017WR021868>
- Lehner, B., Liermann, C. R., Revenga, C., Vörösmarty, C., Fekete, B., Crouzet, P., Döll, P., Endejan, M., Frenken, K., Magome, J., Nilsson, C., Robertson, J. C., Rödel, R., Sindorf, N., & Wisser, D. (2011). High-resolution mapping of the world’s reservoirs and dams for sustainable river-flow management. *Frontiers in Ecology and the Environment*, 9(9), 494–502. <https://doi.org/10.1890/100125>
- Moramarco, T., Barbetta, S., Bjerklie, D. M., Fulton, J. W., & Tarpanelli, A. (2019). River Bathymetry Estimate and Discharge Assessment from Remote Sensing. *Water Resources Research*, 55(8), 6692–6711. <https://doi.org/10.1029/2018WR024220>
- Musa, Z. N., Popescu, I., & Mynett, A. (2015). A review of applications of satellite SAR, optical, altimetry and DEM data for surface water modelling, mapping and parameter estimation. *Hydrology and Earth System Sciences*, 19(9), 3755–3769. <https://doi.org/10.5194/hess-19-3755-2015>
- Neal, J., Schumann, G., & Bates, P. (2012). A subgrid channel model for simulating river hydraulics and floodplain inundation over large and data sparse areas. *Water Resources Research*, 48(11), 1–16. <https://doi.org/10.1029/2012WR012514>
- Oubanas, H., Gejadze, I., Malaterre, P. O., Durand, M., Wei, R., Frasson, R. P. de M., & Domeneghetti, A. (2018). Discharge Estimation in Ungauged Basins Through Variational Data Assimilation: The Potential of the SWOT Mission. *Water Resources Research*, 54(3),

2405–2423. <https://doi.org/10.1002/2017WR021735>

Pujol, L., Garambois, P. A., Finaud-Guyot, P., Monnier, J., Larnier, K., Mosé, R., Biancamaria, S., Yesou, H., Moreira, D., Paris, A., & Calmant, S. (2020). Estimation of multiple inflows and effective channel by assimilation of multi-satellite hydraulic signatures: The ungauged anabranching Negro river. *Journal of Hydrology*, 591(August), 125331. <https://doi.org/10.1016/j.jhydrol.2020.125331>

Revel, M., Ikeshima, D., Yamazaki, D., & Kanae, S. (2020). A framework for estimating global-scale river discharge by assimilating satellite altimetry. *Water Resources Research*, 1–34. <https://doi.org/10.1029/2020wr027876>

Sauer, I. J., Reese, R., Otto, C., Geiger, T., Willner, S. N., Guillod, B. P., Bresch, D. N., & Frieler, K. (2021). Climate signals in river flood damages emerge under sound regional disaggregation. *Nature Communications*, 12(1), 1–11. <https://doi.org/10.1038/s41467-021-22153-9>

Schaperow, J. R., Li, D., Margulis, S. A., & Lettenmaier, D. P. (2019). A Curve-Fitting Method for Estimating Bathymetry From Water Surface Height and Width. *Water Resources Research*, 55(5), 4288–4303. <https://doi.org/10.1029/2019WR024938>

Schellekens, J., Dutra, E., Martínez-De La Torre, A., Balsamo, G., Van Dijk, A., Sperna Weiland, F., Minvielle, M., Calvet, J. C., Decharme, B., Eisner, S., Fink, G., Flörke, M., Peßenteiner, S., Van Beek, R., Polcher, J., Beck, H., Orth, R., Calton, B., Burke, S., ... Weedon, G. P. (2017). A global water resources ensemble of hydrological models: The earth2Observe Tier-1 dataset. *Earth System Science Data*, 9(2), 389–413. <https://doi.org/10.5194/essd-9-389-2017>

WMO (World Meteorological Organisation). (1994). *Guide to Hydrological Practice*.

Weedon, G. P., Balsamo, G., Bellouin, N., Gomes, S., Best, M. J., & Viterbo, P. (2014). The WFDEI meteorological forcing data set: WATCH Forcing data methodology applied to ERA-Interim reanalysis data. *Water Resources Research*, 50(9), 7505–7514. <https://doi.org/10.1002/2014WR015638>

Yamazaki, D., Ikeshima, D., Sosa, J., Bates, P. D., Allen, G. H., & Pavelsky, T. M. (2019). MERIT Hydro: A High-Resolution Global Hydrography Map Based on Latest Topography



- Dataset. *Water Resources Research*, 55(6), 5053–5073.  
<https://doi.org/10.1029/2019WR024873>
- Yamazaki, D., Ikeshima, D., Tawatari, R., Yamaguchi, T., O’Loughlin, F., Neal, J. C., Sampson, C. C., Kanae, S., & Bates, P. D. (2017). A high-accuracy map of global terrain elevations. *Geophysical Research Letters*, 44(11), 5844–5853. <https://doi.org/10.1002/2017GL072874>
- Yamazaki, D., Kanae, S., Kim, H., & Oki, T. (2011). A physically based description of floodplain inundation dynamics in a global river routing model. *Water Resources Research*, 47(4), 1–21. <https://doi.org/10.1029/2010WR009726>
- Yamazaki, D., Lee, H., Alsdorf, D. E., Dutra, E., Kim, H., Kanae, S., & Oki, T. (2012). Analysis of the water level dynamics simulated by a global river model: A case study in the Amazon River. *Water Resources Research*, 48(9), 1–15. <https://doi.org/10.1029/2012WR011869>
- Yamazaki, D., Trigg, M. A., & Ikeshima, D. (2015). Development of a global ~90m water body map using multi-temporal Landsat images. *Remote Sensing of Environment*, 171, 337–351. <https://doi.org/10.1016/j.rse.2015.10.014>
- Yamazaki, D., Revel, M., Zhou, X., & Nitta, T. (2021). global-hydrodynamics/CaMa-Flood\_v4: CaMa-Flood (Version v4.00). Zenodo. <http://doi.org/10.5281/zenodo.4609655>
- Yoon, Y., Durand, M., Merry, C. J., Clark, E. A., Andreadis, K. M., & Alsdorf, D. E. (2012). Estimating river bathymetry from data assimilation of synthetic SWOT measurements. *Journal of Hydrology*, 464–465(2012), 363–375. <https://doi.org/10.1016/j.jhydrol.2012.07.028>
- Zhang, Y., Gao, J., & Gu, Y. (2011). A simple method for mapping bathymetry over turbid coastal waters from MODIS data: possibilities and limitations. *International Journal of Remote Sensing*, 32(22), 7575–7590. <https://doi.org/10.1080/01431161.2010.524903>
- Zhou, X., Polcher, J., & Dumas, P. (2021). Representing Human Water Management in a Land Surface Model Using a Supply/Demand Approach. *Water Resources Research*, 57(4), 1–33. <https://doi.org/10.1029/2020WR028133>
- Zhou, X., Prigent, C., & Yamazaki, D. (2021). Toward Improved Comparisons Between Land-Surface-Water-Area Estimates From a Global River Model and Satellite Observations. *Water Resources Research*, 57(5), e2020WR029256.

<https://doi.org/10.1029/2020WR029256>

Zhou, X., Revel, M., Modi, P., Shiozawa, T., & Yamazaki, D. (2021). Dataset for submission of "Correction of river bathymetry parameters using the stage–discharge rating curve" [Data set]. Zenodo. <http://doi.org/10.5281/zenodo.5006415>